# Dystrophin glycoprotein complex dysfunction

# Dystrophin glycoprotein complex dysfunction: A regulatory link between muscular dystrophy and cancer cachexia

Swarnali Acharyya,[1,2] Matthew E.R. Butchbach,[3] Zarife Sahenk,[4] Huating Wang,[1,2] Motoyasu Saji,[5] Micheal Carathers,[1] Matthew D. Ringel,[1,5] Richard J.E. Skipworth,[6] Kenneth C.H. Fearon,[6] Michael A. Hollingsworth,[7] Peter Muscarella,[8] Arthur H.M. Burghes,[3] Jill A. Rafael-Fortney,[3] and Denis C. Guttridge[1,2,5,*]

[1]Human Cancer Genetics Program, The Ohio State University, Columbus, Ohio 43210
[2]Department of Molecular Virology, Immunology and Medical Genetics, The Ohio State University, Columbus, Ohio 43210
[3]Department of Molecular and Cellular Biochemistry, The Ohio State University, Columbus, Ohio 43210
[4]Department of Neurology, The Ohio State University, Columbus, Ohio 43210
[5]The Arthur G. James Comprehensive Cancer Center, The Ohio State University, Columbus, Ohio 43210
[6]University Department of Surgery, Royal Infirmary, Edinburgh EH16 4SA, United Kingdom
[7]University of Nebraska Medical Center, Omaha, Nebraska 68198
[8]Department of Surgery, The Ohio State University, Columbus, Ohio 43210
*Correspondence: denis.guttridge@osumc.edu

## Summary

**Cachexia contributes to nearly a third of all cancer deaths, yet the mechanisms underlying skeletal muscle wasting in this syndrome remain poorly defined. We report that tumor-induced alterations in the muscular dystrophy-associated dystrophin glycoprotein complex (DGC) represent a key early event in cachexia. Muscles from tumor-bearing mice exhibited membrane abnormalities accompanied by reduced levels of dystrophin and increased glycosylation on DGC proteins. Wasting was accentuated in tumor *mdx* mice lacking a DGC but spared in dystrophin transgenic mice that blocked induction of muscle E3 ubiquitin ligases. Furthermore, DGC deregulation correlated positively with cachexia in patients with gastrointestinal cancers. Based on these results, we propose that, similar to muscular dystrophy, DGC dysfunction plays a critical role in cancer-induced wasting.**

## Introduction

Cachexia is a severe, debilitating consequence of cancer that is estimated to contribute up to a third of all cancer deaths (Argiles et al., 2003; Tisdale, 2002). This syndrome correlates with poor prognosis and severely compromises quality of life. Cachexia physically weakens patients to a state of immobility stemming from anorexia, asthenia, and anemia, and response to standard treatment is usually poor (Andreyev et al., 1998). Wasting results from severe weight loss due to depletion of both adipose tissue and lean muscle mass. However, it is the chronic loss of muscle that most often disrupts the physiological functions of patients, culminating in significantly shortened survival time (van Eys, 1985).

Though the molecular mechanisms of cancer cachexia remain ill defined, research from the last 2 decades has made significant progress on two fronts. First, several mediators have been identified, including proinflammatory cytokines TNFα, IFNγ, and IL-6, as well as the tumor secreted proteolysis-inducing factor (PIF) (Argiles and Lopez-Soriano, 1999; Reid and Li, 2001; Tisdale, 2002). Although the nature and regulation of these cachectic products are distinct, a common mode of action in mediating wasting is through the loss of myofibrillar proteins, in particular myosin heavy chain (MyHC) (Acharyya et al., 2004). Second, cachexia mediators reduce lean muscle mass by altering the homeostasis between synthesis and degradation of muscle protein (Rennie et al., 2004). Protein degradation is largely regulated by the lysosomal and ubiquitin proteasome pathways (Farges et al., 2002; Hasselgren and Fischer, 2001; Jackman and Kandarian, 2004; Lecker et al., 1999). Genes regulating proteasome-mediated proteolysis are elevated in muscles from animal models of cancer cachexia as well as in patients (Temparis et al., 1994; Williams et al., 1999). Identification of two muscle-specific E3 ubiquitin ligases, MuRF1 and

### SIGNIFICANCE

**Cachexia, or muscle wasting, is a debilitating consequence of cancer. Although this syndrome is often related to late-stage disease, effective cachexia therapy may improve patient response to cancer treatment, impacting quality of life and survival. We find that wasting in cancer is linked to a dysfunctional dystrophin glycoprotein complex (DGC), a membrane structure associated with muscular dystrophy. Tumor progression leads to dystrophin reduction and aberrant DGC glycosylation. Tumor-induced muscle wasting is also enhanced in dystrophin null mice but spared in dystrophin transgenic animals. Furthermore, DGC deregulation is also present in cachectic patients with gastroesophageal adenocarcinoma. Thus, DGC dysfunction is an underlying cause of wasting in both muscular dystrophy and cancer, a finding that may prove useful for anticachexia therapy.**

atrogin-1/MAFbx, have further demonstrated the predominant contribution of the proteasome pathway in muscle wasting (Bodine et al., 2001; Gomes et al., 2001). Furthermore, Foxo transcription factors were recently shown to regulate expression of these ligases in various models of atrophy (Sandri et al., 2004; Stitt et al., 2004). However, despite these insights into the molecular etiology of this syndrome, effective cancer cachexia therapy remains elusive.

A separate group of muscle disorders also characterized by severe muscle wasting are the muscular dystrophies. Duchenne/Becker and several forms of limb-girdle muscular dystrophy are linked to mutations in genes that encode components of the dystrophin glycoprotein complex (DGC), a multiprotein structure associated with myofiber membranes (Dalkilic and Kunkel, 2003; Durbeej and Campbell, 2002; Blake et al., 2002). At the core of the DGC is dystrophin, a large 427 kDa protein associating with the cytoskeleton through interaction with F-actin at its amino terminus and connection to the sarcolemma by binding to β-dystroglycan (β-DG) at its carboxyl end (Ervasti et al., 1990; Hoffman et al., 1987; Yoshida and Ozawa, 1990). β-DG is bound to α-dystroglycan (α-DG), which itself is linked to the extracellular matrix by its interactions with laminin-2. The DGC therefore forms a strong mechanical link between the cytoskeleton and the extracellular matrix, protecting cells from contraction-induced injuries (Campbell and Stull, 2003). In addition, the DGC maintains an active signal transduction pathway by interacting with Grb2 and nNOS (Rando, 2001). Mutations in dystrophin or other members of the DGC disrupt the mechanical linkage and/or signaling pathway(s), resulting in membrane damage, necrosis, and eventual muscle wasting (Lapidos et al., 2004).

Although the underlying mechanisms of muscle cachexia appear nonoverlapping to those in muscular dystrophy, our current findings suggest that a dysfunctional DGC might be a common link between these two disease states.

## Results

### Murine models recapitulate histological features of human cancer cachexia

To gain insight into the mechanisms underlying muscle wasting in cancer, we performed histological analysis of cachectic muscles in tumor-bearing mice. In biopsies from cancer patients, wasting results from atrophy selectively in type II fibers. Increased vascularization is observed, but overt signs of inflammation or apoptosis are typically absent (Karpati and Carpenter, 2001; Marin and Denny-Brown, 1962; Mendell and Engel, 1971). Similarly, muscles from mice bearing subcutaneous colon-26 (C-26) tumors were severely atrophic, exhibiting 45% reduction in mean fiber diameter in tibialis anterior (TA) (Figure 1A), with similar atrophy observed in gastrocnemius (Figure 1A) and quadriceps (data not shown). Myofibrillar ATPase staining of the mixed fiber type gastrocnemius muscle confirmed that atrophic fibers were selectively type II in origin (Figure 1B). Mean diameter reductions of these fibers were 40% (40.8 ± 0.3 μm in control compared to 24.3 ± 0.2 μm in tumor-bearing mice), while type I fibers remained relatively unchanged (35.7 ± 0.4 μm in controls to 36.9 ± 0.4 μm in tumor mice) (Figure 1C). ATPase staining also revealed the presence of increased blood vessels in cachectic muscles, which was confirmed by the endothelial cell-specific marker von Willebrand factor (Figure 1A).

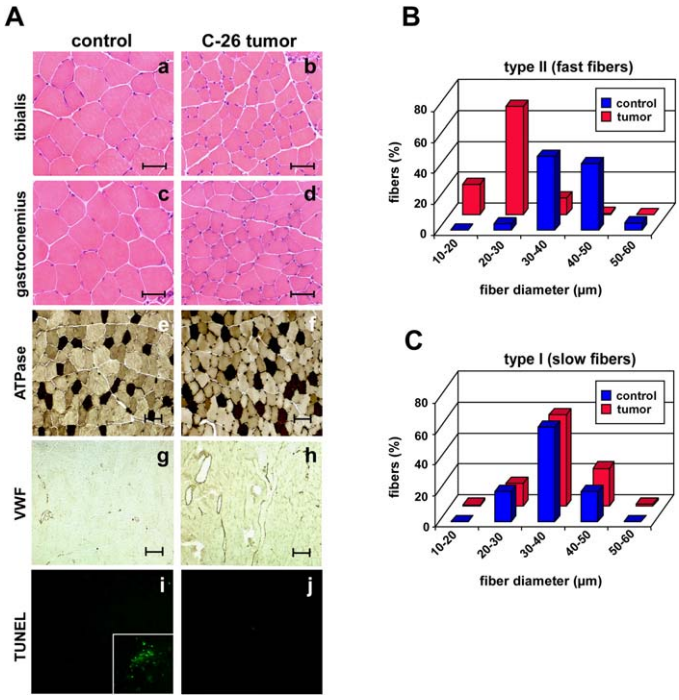


**Figure 1.** Histological features of the C-26 murine model of cancer cachexia

**A:** H&E-stained cryosections of TA (**Aa** and **Ab**) and gastrocnemius (**Ac** and **Ad**) muscles were analyzed from control mice or mice injected with C-26 cells after 25 days (scale bar, 25 μm). Gastrocnemius sections (**Ae** and **Af**) were stained with myofibrillar ATPase (pH 4.6) to differentiate slow (type I, dark) and fast (type II, intermediate to light staining) fibers (scale bar, 50 μm). Immunohistochemical analysis of muscle sections with antibody against von Willebrand factor (VWF) in saline- or tumor-injected mice (**Ag** and **Ah**) (scale bar, 100 μm). TUNEL assays were performed on muscle sections (**Ai** and **Aj**) using thymus as positive control (inset).

**B:** Fiber diameter was measured from muscle sections stained with ATPase from control and C-26 tumor mice (n = 3 each) at 25 days.

**C:** Similar analysis as in **B** was repeated with type I fibers.

Although infiltration of inflammatory cells is often a consequence of increased vascularization, no statistically significant differences were observed in the numbers of lymphocytes or macrophages between control and C-26 muscles (data not shown). Moreover, TUNEL staining revealed little if any evidence of apoptosis (Figure 1A). Taken together, our analysis suggest that the C-26 model faithfully recapitulates the clinical features of cancer-induced muscle wasting (Karpati and Carpenter, 2001), indicating that the mechanisms regulating muscle breakdown in this murine model are likely to overlap with those present in the human condition.

### Cachectic fibers show abnormal membrane morphology

Upon closer histological examination, alterations in membrane structure were apparent in muscles from C-26 tumor-bearing mice. As compared to the smooth and well-defined membrane bordering each myofiber in control muscles, membranes in cachectic muscles appeared wrinkled and irregular (Figure 2A). This phenotype was confirmed by electron microscopy and laminin staining, giving an early indication that sarcolemma and the associated basal lamina from cachectic muscles were ab-

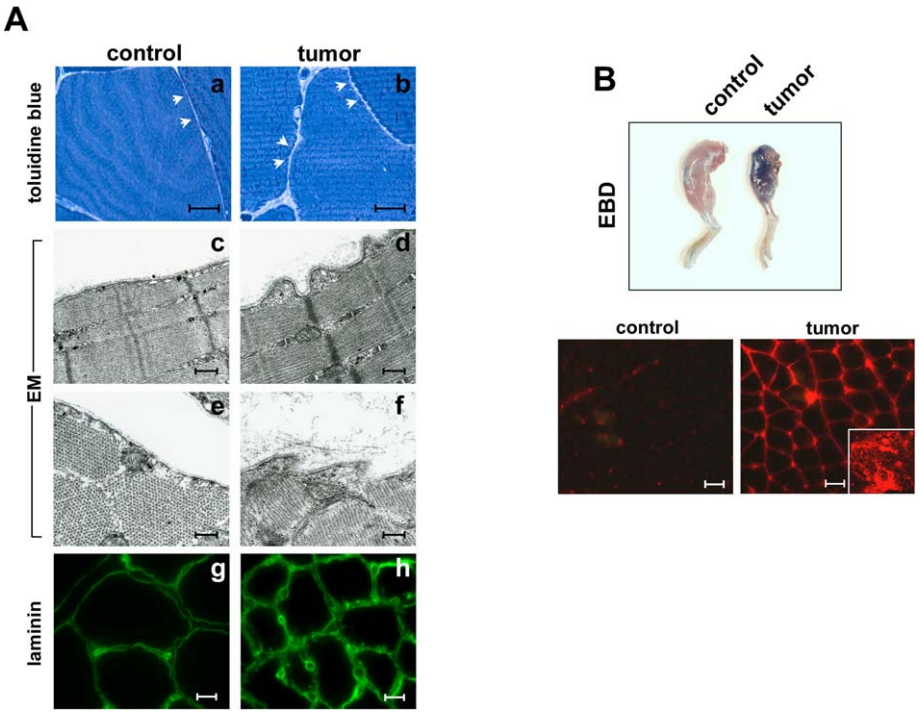


**Figure 2.** Tumor-bearing mice exhibit abnormal muscle membranes

**A:** Muscles from control (**Aa**) or mice bearing tumors (**Ab**) for 20 days were stained with toluidine blue (arrowheads denote fiber edge; scale bar, 2.5 μm). Ultrathin sections of control and tumor-bearing mice were analyzed by EM (**Ac**–**Af**) (scale bar, 0.2 μm). Longitudinal sections (**Ad**) revealed normal Z band streams in cachectic muscles, while cross-sections (**Af**) showed evidence of myofibrillar disarray. Laminin immunofluorescence was performed on sections from control (**Ag**) or C-26-bearing (**Ah**) mice (scale bars = 10 μm).

**B:** Control and C-26 tumor mice were injected intraperitoneally with EBD for 24 hr. Gross morphology of hindlimb was examined (top panel), and sections of TA muscles were subsequently prepared and visualized by fluorescence; scale bar, 100 μm (inset depicts EBD-filled fibers).

normal (Figure 2A). Such morphological changes raised the intriguing possibility that membrane damage could be associated with the pathogenesis of cancer cachexia. To test this, Evans blue dye (EBD) uptake was used to measure membrane integrity. EBD is normally membrane impermeable, but in damaged myofibers this dye penetrates the sarcolemma and accumulates in the cytoplasm (Straub et al., 1997). Gross morphological analysis of muscles from tumor mice injected with EBD revealed visibly higher uptake of the dye over that in control mice (Figure 2B). To determine the precise dye localization, TA muscles were sectioned and histologically examined. Consistent with gross analysis, muscles from cachectic mice absorbed greater amounts of dye, and in some, albeit rare sections, dye infiltration occurred in the cytoplasm of clustered myofibers. Dye uptake did not simply result from increased vasculature in cachectic muscles, since uptake was negligible in both TA and the more highly vascular soleus muscles in control mice (Figure S1 in the Supplemental Data available with this article online). Serum creatine kinase (CK) is also used as an indicator of weakened membranes (Durbeej and Campbell, 2002). However, in C-26-bearing mice CK levels were only moderately elevated over that of controls (Figure S1), indicating that although tumor burden causes alterations to muscle membranes or associated basal lamina, the severity of this damage is not sufficient to cause a complete permeation of EBD or release of intracellular proteins.

### Regulation of the DGC is associated with cancer cachexia

The DGC plays a major role in regulating membrane integrity, and mutations in this complex result in different forms of muscular dystrophies (Campbell and Stull, 2003). Although the causative mechanisms of muscular dystrophies and cachexia are considered distinct, given the membrane irregularities observed in tumor-bearing mice, we considered that the DGC might also be involved in the regulation of cancer cachexia. To initiate this analysis, we examined the potential regulation of the DGC core member, dystrophin. Western analysis revealed that dystrophin was reduced in muscles from tumor-bearing mice (Figure 3A) at a time that preceded reductions in mean fiber diameter (Figure 7B). Immunofluorescence further showed that, in comparison to the uniform staining of control fibers, dystrophin expression in tumor mice was discontinuous or completely absent along the sarcolemma of many fibers (Figure 3B). Changes at the protein level did not correlate with mRNA (Figure 3A), suggesting that downregulation of dystrophin in tumor-bearing mice is posttranscriptional. In Duchenne muscular dystrophy (DMD), loss of dystrophin is often associated with compensatory upregulation of its autosomal homolog utrophin (Tinsley et al., 1998). Muscles from tumor-bearing mice showed similar induction of utrophin, which by Western resolved as two forms (Figures 3A and 3B). Although the nature of these forms requires further characterization, the results nevertheless support the deregulation of dystrophin in cachectic muscles. Conditions where dystrophin expression is lost, such as in muscular dystrophies or enterovirus-mediated cardiomyopathy, typically result in the concurrent downregulation of other DGC members (Badorff et al., 1999; Durbeej and Campbell, 2002). This was not the case in cancer cachexia, since expression of α-DG, β-DG, α-sarcoglycan (SG), β-SG, δ-SG, and dysferlin was unaltered (Figure 3C), and changes were not detected in caveolin-3, syntrophin, and Grb2 (data not shown).

Prominently detected in muscles from tumor-bearing mice, however, was the presence of a higher migrating band for both β-DG and β-SG (Figure 3C). Since aberrant posttranslational

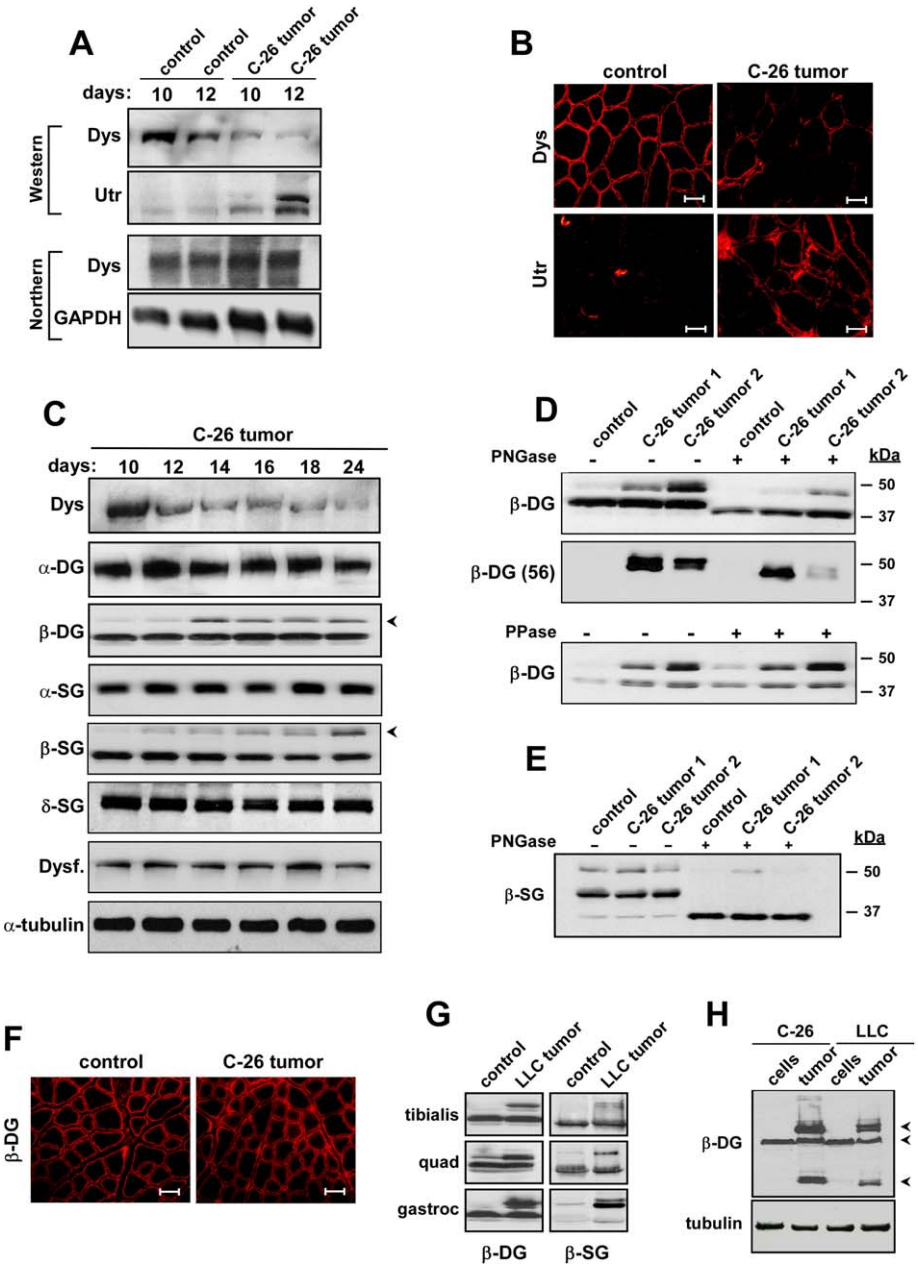


**Figure 3.** Tumor-induced alterations in the DGC

**A:** Analysis of dystrophin (Dys) and utrophin (Utr) by Westerns or Dys and GAPDH by Northerns from TA muscles harvested at indicated days following either saline (control) or C-26 tumor cell injections.

**B:** Immunofluorescence on TA muscles from day 12 control and C-26 tumor mice stained with Dys and Utr (scale bar, 20 μm).

**C:** TA muscles were collected from C-26 tumor mice at indicated days, and immunoblots were performed probing for DGC members: Dys; α- and β-DG; α-, β-, and δ-SG; dysferlin (Dysf); and α-tubulin as loading control. Arrowheads indicate higher migrating forms of β-DG and β-SG.

**D:** Tissue lysates from control and cachectic muscles were either untreated (−) or treated (+) with PNGaseF or λ-phosphatase (PPase) and subsequently probed for β-DG with C-terminal (Novacastra) or N-terminal (BD, clone 56) antibodies.

**E:** Western for β-SG in C-26 lysates untreated or treated with PNGaseF.

**F:** Immunofluorescence staining for β-DG in TA sections from day 14 control and C-26 tumor mice (scale bar, 50 μm).

**G:** Westerns for β-DG and β-SG in TA, quadriceps (quad), and gastrocnemius (gastroc) muscles from saline (control)- and LLC-injected mice.

**H:** Western for β-DG in C-26 and LLC cultured cells and tumors, with tubulin used as a loading control. Arrows indicate β-DG-processed (lower), endogenous (middle), and hyperglycosylated (top) forms.

glycosylation of dystroglycan proteins is known to occur in various disease states (Jing et al., 2004; Michele et al., 2002), we investigated the possibility that β-DG and β-SG were subjected to a similar deregulation in cancer cachexia. Consistent with previous findings, treatment of control muscle lysate with glycosidase PNGaseF decreased the 43 kDa basally glycosylated form of β-DG by approximately 5 kDa (Holt et al., 2000) and, as also reported, caused a nonspecific reduction of β-DG (Esapa et al., 2003) (Figure 3D). In cachectic muscles, the 43 kDa form of β-DG was also shifted with PNGaseF, but importantly, so was the higher form. In addition, the almost complete disappearance of the higher migrating band corresponded with a concomitant increase of endogenous protein, suggesting that this higher band represents a hyperglycosylated form of β-DG. A decrease in the higher form was also detected when PNGaseF-treated lysates were probed with either a β-DG antibody generated to the identical epitope in the carboxyl terminus (MANDAG 2, clone 7D11) (data not shown) or with an amino-terminal antibody that favored recognition of the higher form (clone 56) (Figure 3D). It is possible that other posttranslational modifications occur in β-DG, but such modifications are not due to phosphorylation, since no change in β-DG mobility was observed when lysates were treated with phosphatase (Figure 3D). In an analogous fashion, PNGaseF-sensitive glycosylation was also reproducibly detected in the higher form of β-SG (Figure 3E). The fact that no alterations were detected in other glycosylated DGC members, α-SG and δ-SG (Figure 3C), or non-DGC glycosylated proteins such as β1 subunit of

ATPase and NCAM (Figure S2), argued that aberrant glycosylation of β-DG and β-SG was specific to these DGC proteins. Furthermore, although alterations in glycosylation can result in abnormal trafficking of DGC proteins (Holt et al., 2000), altered glycosylation of β-DG and β-SG did not appear to affect the cellular localization of these proteins (Figure 3F). To evaluate if these findings could be extended to another model of cancer cachexia, β-DG and β-SG were monitored in mice bearing Lewis lung carcinoma (LLC). Consistent with C-26 tumors, LLC promoted altered glycosylation of β-DG and β-SG in various muscle groups (Figure 3G), correlating with reduced muscle mass and decreased dystrophin expression (Figure S2). Since β-DG processing is associated with cellular transformation (Jing et al., 2004), we also analyzed whether a similar deregulation occurred in C-26 and LLC tumors. Results showed that, although such processing did occur, interestingly, hyperglycosylation of β-DG was also apparent in tumors, but not cultured cells (Figure 3H), indicating that tumor communication with the microenvironment or distant target tissues is required for modifications of this DGC protein. Collectively, these results demonstrate that alterations in the DGC are characteristic of a tumor-induced wasting state.

**Regulation of the DGC is specific to cachectic fibers**

Having established a potential link between the DGC and tumor-regulated muscle wasting, we next sought to address whether DGC regulation was selective to atrophic fibers. For this determination, laser capture microdissection (LCM) was performed on muscle sections from control and C-26 tumor-bearing mice. In order to test the validity of this approach, β-DG Westerns were performed comparing LCM-captured fibers to muscle homogenates. As with tissue homogenates, a clear increase in hyperglycosylation of β-DG was detected in cachectic fibers isolated by LCM (Figure 4A). Next, LCM was used to compare DGC proteins between cachectic and non-cachectic fibers captured from the same wasted muscle. Results showed reproducibly higher intensity of β-DG and β-SG glycosylation in fibers deemed cachectic by a mean diameter of less than 30 μm (Figure 4B; dotted boundary). In comparison, troponin expression was unaltered among these fiber groups. Since tumor-induced atrophy is selective to type II fibers (Figure 1), we investigated if DGC alterations were fiber type specific. C-26 derived gastrocnemius muscles were sectioned and subsequently stained for myosin ATPase or slow MyHC to distinguish type I from type II fibers. LCM was then performed on serial sections, and Westerns were repeated. Results showed that, although a faint hyperglycosylated form of β-DG appeared in type I fibers (most likely reflecting type II fibers present within type I groupings), this glycosylation pattern was noticeably enhanced in captured type II fibers (Figure 4C). To verify this selectivity, double immunofluorescence of dystrophin and MyHC-I was performed on sections from tumor-bearing mice. Results showed that, although some reduction in dystrophin occurred in type I fibers, the predominant reduction was type II associated (Figure 4D). Together, these data suggest that regulation of the DGC is selective to the atrophic state of type II fibers in response to tumor burden.

**Tumor-induced functional loss of the DGC**

To understand the functional relevance of DGC regulation, we assessed binding interactions between DGC proteins from

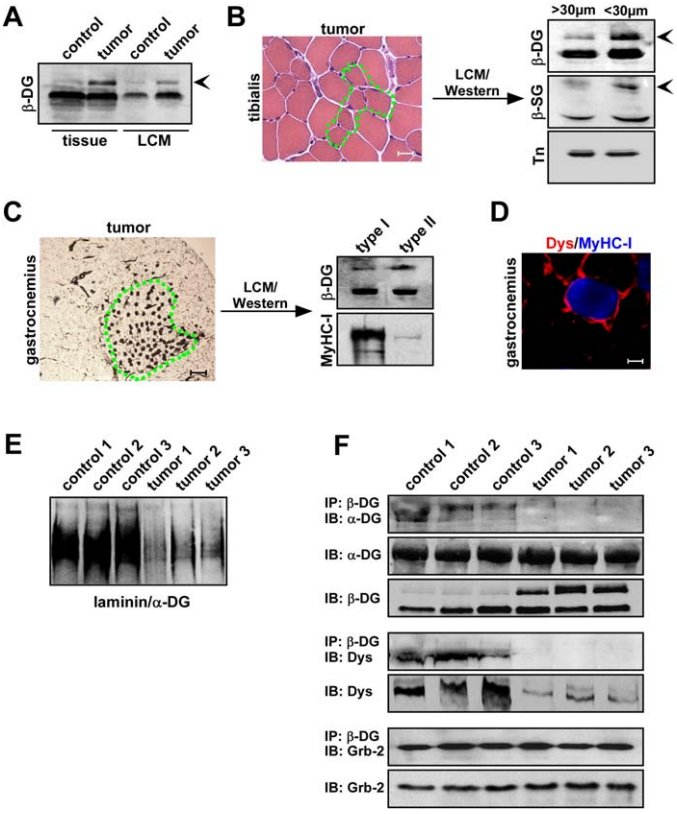


**Figure 4.** DGC alterations are selective to cachectic fibers and lead to loss of interactions

**A:** β-DG Westerns from control and tumor mice detected from tissue lysates or lysates prepared from approximately 5000 muscle fibers captured by LCM. Arrowhead marks altered β-DG glycosylation.

**B:** LCM was performed based on fiber size from TA muscles of tumor-bearing mice (dotted boundary represents fibers <30 μm in diameter) (scale bar, 25 μm), followed by Westerns for β-DG, β-SG, and troponin (Tn). Arrowheads indicate hyperglycosylation.

**C:** Areas for microdissection were selected upon staining sections of gastrocnemius muscles from tumor mice with ATPase (pH 4.2) stain (dotted boundary represents type I fibers) (scale bar, 200 μm). LCM was performed on serial sections, and β-DG and MyHC type I were subsequently probed by Westerns.

**D:** Double immunofluorescence of muscle from day 10 C-26-injected mice with dystrophin (red) and MyHC type I (blue) (scale bar, 10 μm).

**E:** Ligand overlay assays performed on WGA-enriched muscle homogenates from control and C-26 tumor mice.

**F:** Coimmunoprecipitations (IP) were performed using a β-DG antibody, and interacting proteins were detected by immunoblotting (IB) probing for α-DG, dystrophin (Dys), and Grb-2. Levels of proteins are shown by corresponding Westerns.

control and tumor mice. In the DGC, α-DG serves as a receptor binding laminin-2 in the extracellular matrix (Campbell and Stull, 2003). Using ligand overlay assays, a significant reduction in laminin-α-DG binding was observed in C-26 cachectic muscles (Figure 4E). Furthermore, coimmunoprecipitation analysis revealed pronounced decreases in interactions between α-DG and β-DG and between β-DG and dystrophin in tumor mice (Figure 4F). Corresponding Westerns confirmed that loss of interactions was associated with decreases in dystrophin and alterations in β-DG. Regulation of DGC interac-

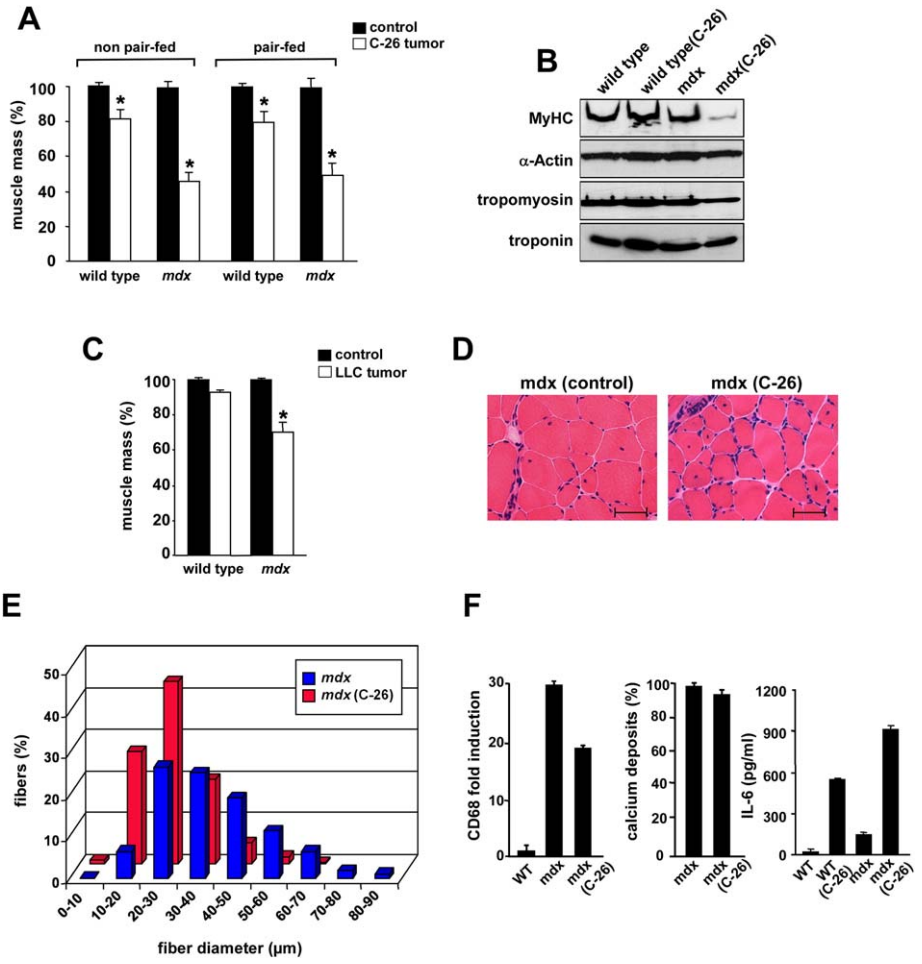


**Figure 5.** Wasting is enhanced in tumor-bearing *mdx* mice

**A:** Saline or C-26 tumor cells ($5 \times 10^5$ cells) were injected subcutaneously into the right flank of C57BL/10/CD2F1 (wild-type) or *mdx*/CD2F1 male mice with (n = 6) or without (n = 8) pair feeding. After 2–3 weeks, gastrocnemius muscles were weighed. Muscle mass loss from tumor mice was expressed as a percentage of controls, which was set to a value of 100% (asterisk denotes statistically significant differences, $p < 0.05$; similar statistically significant results were obtained with TA and quadriceps muscles).

**B:** Westerns probing for myofibrillar proteins from wild-type and *mdx* mice with and without C-26 tumors after 14 days.

**C:** Muscles from C57BL/6 or *mdx*/C57BL/6 mice injected intramuscularly with either saline control or LLC cells were weighed and harvested after 14 days. Mass from LLC muscles is expressed as percentage of controls, which was set at 100% (asterisk denotes $p < 0.05$).

**D:** H&E stains of gastrocnemius muscle from 6-week-old *mdx* or *mdx* mice bearing C-26 tumors for 14 days (scale bar, 50 μm).

**E:** Fiber diameter was measured from H&E sections in **D**.

**F:** Real-time RT-PCR of CD68 from wild-type, saline-injected, or C-26 tumor *mdx* mice. Percent calcifications of muscles stained with von Kossa from *mdx* mice injected with saline (set at 100%) and C-26 tumor cells. IL-6 ELISA from serum of wild-type and *mdx* mice with and without tumors.

For graphs, data are plotted as mean ± SEM.

tions appeared selective, since no change in the affinity of β-DG and Grb2 was detected. These results show that tumor-induced muscle wasting correlates with dissociation of the DGC along the extracellular matrix-cytoskeleton axis, possibly resulting from the deregulation of dystrophin, β-DG, and β-SG.

**Loss of DGC enhances cancer-induced muscle atrophy**

To firmly establish the contribution of the DGC in cancer cachexia, we took advantage of the *mdx* murine model of DMD. *mdx* mice have a mutation that codes for a premature stop codon in the X-linked dystrophin gene (Sicinski et al., 1989) resulting in the loss of dystrophin and associated DGC proteins (Ohlendieck and Campbell, 1991). Although the *mdx* pathology resembles the early phases of DMD, relatively little muscle loss actually occurs in these mice due to the high rate of muscle regeneration and hypertrophy in response to the ongoing cycles of degeneration (Durbeej and Campbell, 2002). Thus, C57/BL10 *mdx* mice were crossed into a CD2F1 background, and C-26 tumors were administered to wild-type and *mdx* males. Although mice exhibited comparable tumor burden, muscle loss was accentuated in *mdx*/CD2F1 mice compared to wild-type C57BL10/CD2F1 littermates (Figure 5A). Daily cage monitoring indicated that muscle loss in *mdx* mice was not due to asthenia or anorexia (Figure S3), and consistent with this latter observation, muscle wasting was also enhanced in *mdx* mice over wild-type in pair-fed conditions (Figure 5A). Greater reduction in muscle mass correlated with a decrease in MyHC (Figure 5B), indicative of a bona fide wasting state, and as previously described (Acharyya et al., 2004) this regulation was selective over other core myofibrillar proteins. Importantly, fiber membranes from *mdx* mice alone were visibly irregular, and DGC proteins were also aberrantly glycosylated (Figure S4), suggesting that loss of dystrophin leads to β-DG and β-SG alterations. Furthermore, these effects were not restricted to the C-26 model, since a significant decrease in muscle mass also occurred in *mdx* mice bearing LLC tumors (Figure 5C).

To elucidate how the loss of DGC in *mdx* mice exacerbated muscle wasting in response to tumor factors, histological analysis was performed. Consistent with reduced mass, fibers from C-26 *mdx* mice exhibited substantial atrophy with an average fiber diameter reduction of 33% (40.0 ± 0.46 μm in controls compared to 26.9 ± 0.21 μm in *mdx* tumor mice) (Figures 5D and 5E). Since inflammation and abnormal calcium influx are considered important mediators of wasting in DMD (Blake et al., 2002), we assessed whether these factors were responsible for the increased muscle loss in the tumor-bearing state. As reported (Chen et al., 2000), the CD68 inflammatory

marker was pronouncedly elevated in *mdx* mice, but no further regulation occurred in mice with C-26 tumors (Figure 5F). Similarly, no differences were seen in dystrophic calcifications between tumor and nontumor *mdx* animals. Tumor *mdx* mice did, however, exhibit higher circulating levels of IL-6, consistent with suspected involvement of this cytokine in C-26-mediated atrophy (Argiles and Lopez-Soriano, 1999). These data therefore suggest that loss of the DGC exacerbates tumor-induced wasting resulting from an atrophic rather than a dystrophy-associated condition.

### Muscle-specific dystrophin expression blocks tumor-induced muscle wasting

Next, we reasoned that, if a dysfunctional DGC is relevant in cancer cachexia, restoration of this complex would rescue the cachectic phenotype in response to tumor burden. To test this, transgenic mice expressing a dystrophin minigene in skeletal muscle (Δ17-48) (Phelps et al., 1995) were crossed into a CD2F1 background, and C-26 tumors were administered. As with *mdx* mice, tumor growth and food intake (Figure S5) were comparable between wild-type and Δ17-48 animals. However, while appreciable muscle mass was lost in wild-type mice, little to no decrease in mass and fiber diameter occurred in dystrophin transgenic mice (Figures 6A and 6B). EM and laminin staining also revealed that muscles from Δ17-48 tumor mice were spared of membrane abnormalities, and overlay assays showed restored DGC interactions (Figures 6C and 6D). Furthermore, assessment of muscle function showed that wild-type mice with tumors had approximately 30% reduction in hindlimb grip strength (1.02 ± 0.14 N for controls and 0.70 ± 0.15 N for C-26 tumor mice) (Figure 6E), while no differences were observed between control and dystrophin transgenic mice (0.94 ± 0.24 N to 0.93 ± 0.13 N, respectively). Taken together, these results argue that DGC restoration can both structurally and functionally block tumor-induced muscle changes.

### DGC dysfunction mediates the induction of muscle E3 ubiquitin ligases

To assess the significance of a dysfunctional DGC in cachexia, we examined whether other factors involved in the maintenance of muscle mass were equally affected by a tumor burden state. Although studies support the role of PI(3)K/Akt signaling in regulating muscle hypertrophy (Glass, 2003), at least in the C-26 model no significant differences in activated Akt were detected in either gastrocnemius or TA (Figure 7A and data not shown), nor were changes seen in MAPK. Cachectic muscles, however, displayed a pronounced increase in p70S6K activity that might have been due to the accumulation of amino acids released from catabolized proteins (Liu et al., 2004). Another signaling pathway whose activation has been shown to be required for muscle wasting is NF-κB (Cai et al., 2004; Guttridge et al., 2000; Hunter and Kandarian, 2004). Consistent with these findings, NF-κB activity was also reproducibly elevated in cachectic muscles over that of controls (Figure 7A). Among the degradation pathways, the ubiquitin proteasome system regulates muscle atrophy via the induction of muscle E3 ligases in various catabolic states including cancer (Lecker et al., 2004), and E3 ligase requirement has been demonstrated in response to glucocorticoid treatment (Bodine et al., 2001), and more recently to chronically stimulated NF-κB signaling (Cai et al., 2004). To further investigate the role of the proteasome system in tumor-bearing mice, we performed a time course analysis of E3 expression in relation to the onset of muscle atrophy. Results showed that MuRF1 was induced within 10 days following tumor cell inoculum, preceding the initial reduction in fiber size (Figure 7B). Interestingly, this induction occurred around the same time that alterations in the DGC were detected (Figure 3). This raised the intriguing possibility that DGC dysfunction may either regulate or be itself regulated by the proteasome. To test this, MuRF1 expression and

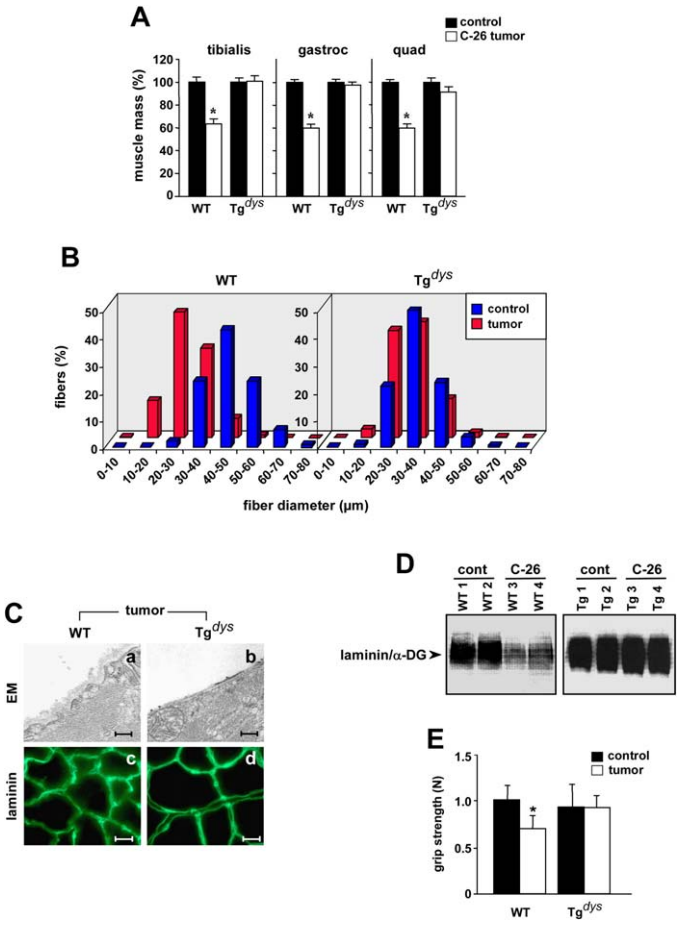


**Figure 6.** Wasting is spared in tumor-bearing dystrophin transgenic mice

**A:** TA, gastrocnemius (gastroc), and quadriceps (quad) muscles from wild-type (C57BL/10/CD2F1; WT) and Δ17-48/CD2F1 transgenic ($Tg^{dys}$) mice injected with either saline alone (control) or C-26 cells were harvested and weighed 20–21 days after injection (minimum of n = 6 for each group). Muscle loss is expressed as a percentage of control muscle mass, set to a value of 100% (asterisk denotes $p < 0.05$).

**B:** Fiber diameter of gastrocnemius muscles from mice shown in **A** (similar results were obtained with TA and quadriceps muscles).

**C:** Cross-sections of muscles from wild-type (**Ca**) or Δ17-48/CD2F1 transgenic (**Cb**) mice both bearing tumors were prepared and analyzed by EM (scale bar, 0.2 μm), or sections from wild-type (**Cc**) and dystrophin transgenic mice (**Cd**) were stained for laminin (scale bar, 20 μm).

**D:** Muscles from mice as in **C** were homogenized, and laminin overlay assays were performed (cont, control).

**E:** Hindlimb grip strengths for wild-type (WT) and Δ17-48/CD2F1 transgenic ($Tg^{dys}$) mice injected with PBS (control) or C-26 tumor cells (asterisk denotes $p = 0.051$).

For graphs, data are plotted as mean ± SEM.

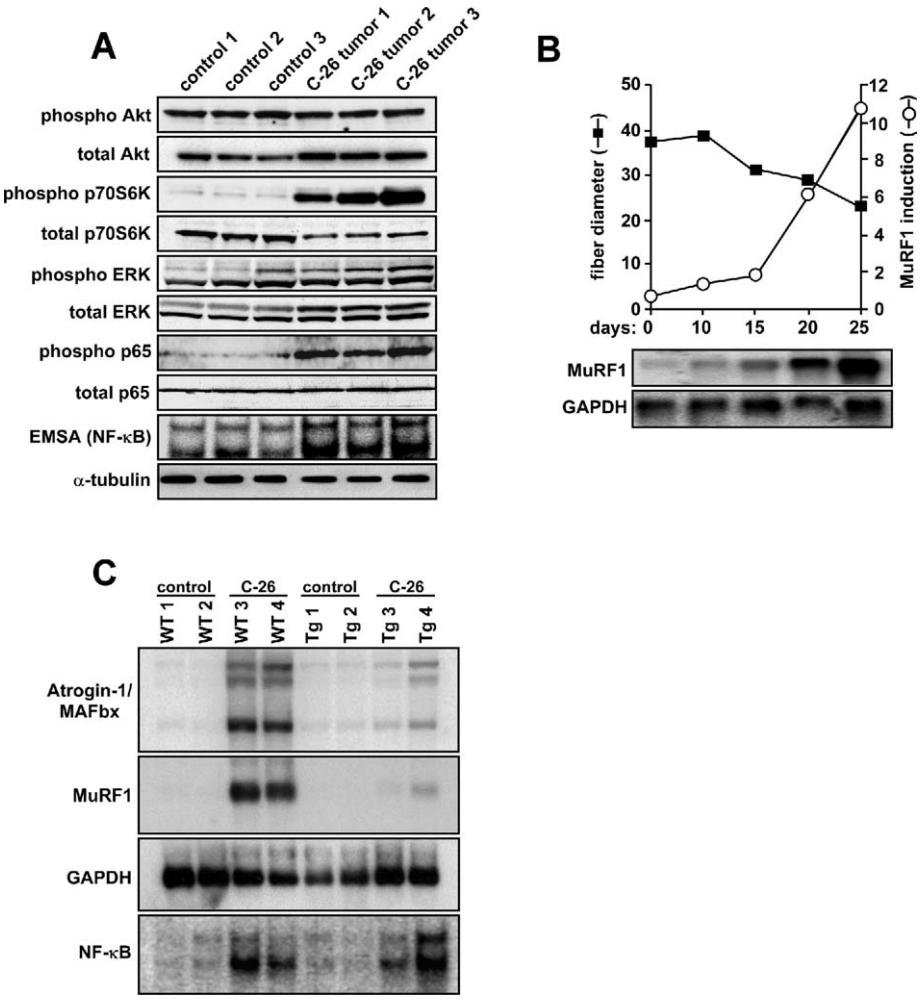


**Figure 7.** Tumor-induced ubiquitin ligase expression is blocked in dystrophin transgenic mice

**A:** Gastrocnemius muscles from saline- and C-26-injected CD2F1 mice after 20 days were homogenized and examined by immunoblots probing for indicated signaling proteins and tubulin as a loading control, or examined by EMSA for NF-κB activity.

**B:** Northern of MuRF1 in muscles isolated from tumor mice at indicated days. Expression of MuRF1 was quantitated by phosphoimaging and normalized to GAPDH. The degree of MuRF1 induction was plotted against the percentage of muscle atrophy determined by measuring fiber diameter on the same days.

**C:** Northern (MuRF1, atrogin-1/MAFbx, GAPDH) and EMSA (NF-κB) analyses from muscles of C57BL/10/CD2F1 wild-type or Δ17-48/CD2F1 dystrophin transgenic mice injected with either saline (control) or C-26 tumor cells (n = 9).

atrogin-1/MAFbx expression were examined in tumor-bearing C57BL10/CD2F1 wild-type and dystrophin Δ17-48 transgenic animals. Results showed that while both E3 ligases were strongly induced in wild-type mice, this regulation was substantially reduced in muscles with rescued DGC (Figure 7C; observed in 7/9 tumor-bearing transgenics). In contrast, NF-κB was increased in both C-26 tumor-bearing wild-type and dystrophin transgenic mice. Collectively, results imply that DGC dysfunction regulates the ubiquitin proteasome system in an NF-κB-independent manner.

**DGC is deregulated in cancer patients with cachexia**

Finally, we addressed whether DGC dysfunction was present in patients with cancer cachexia. DGC was examined in muscle biopsies from patients with gastrointestinal cancers, since such patients commonly undergo extensive weight loss (Andreyev et al., 1998) and demonstrate poor quality of life and reduced survival (Deans and Wigmore, 2005). Compared to weight-stable healthy controls, results showed that carcinoma patients with marked weight loss had dramatic reductions in dystrophin (Figure 8A; Table S1). Ponceau S staining confirmed that this loss was not due to a general reduction in total protein. In the murine models of cachexia, decreases in dystrophin were associated with increased glycosylation of β-DG and β-SG. Likewise, dystrophin reduction in patients was tightly linked with hyperglycosylation of DGC proteins, to the extent that a direct correlation was clearly discernable between dystrophin reduction and β-DG and β-SG glycosylation (termed deregulated DGC).

A more extensive analysis from 14 control individuals and 27 histologically confirmed gastroesophageal adenocarcinoma (ACC) patients (11 esophageal, 12 stomach, 4 esophagogastric junction) revealed that DGC deregulation was completely absent in controls but present in 16 (59%) ACC samples, thus indicating a disease association. Significantly, when stringent parameters of cachexia were applied, defined by C-reactive protein levels > 10 mg/l and weight loss > 10% of preillness weight (Deans and Wigmore, 2005), 10/11 (91%) patients exhibited prominent DGC deregulation ($\chi^2 = 5.593$; df = 1; p = 0.02) (Figure 8B). Equally striking was that, of ten nonsurviving cases, 10/10 (100%) were also positive DGC deregulation. Kaplan-Meier survival analysis demonstrated a statistically significant difference between normal and deregulated DGC cases (p = 0.006 by log rank test) (Figure 8C). Moreover, analogous to the C-26 model, ligand overlay assays from carcinoma patients revealed decreases in DGC association (Figure 8D).

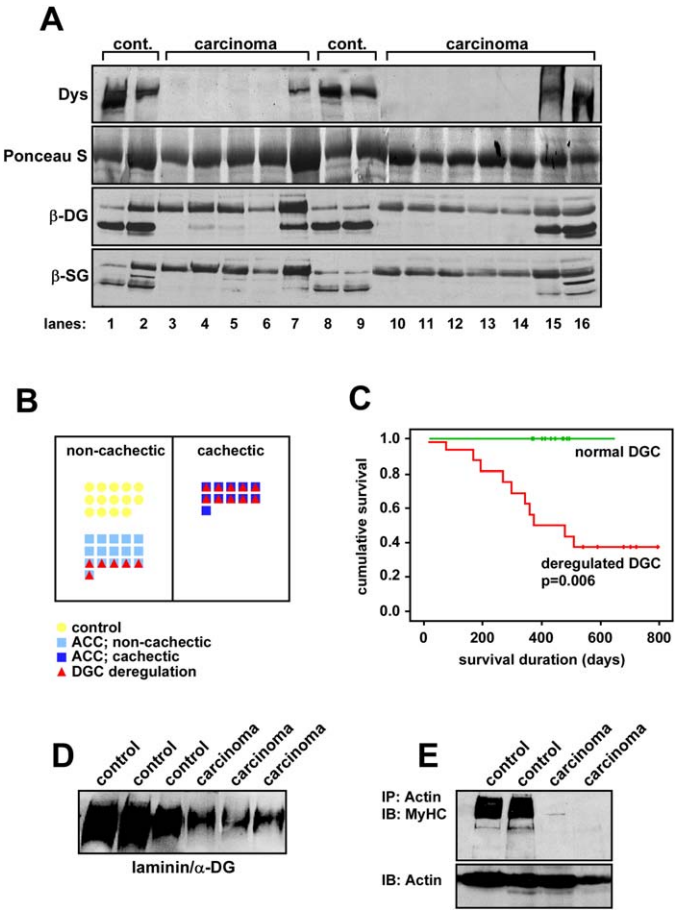


**Figure 8.** DGC dysfunction is associated with cachexia in gastrointestinal carcinoma patients

**A:** Rectus abdominus biopsies from control (cont.) and adenocarcinoma patients were homogenized and analyzed by Westerns probing for Dys, β-DG, and β-SG. Upper band denotes hyperglycosylated products.

**B:** The relationship between cachexia and survival with DGC deregulation in healthy control (n = 14) and ACC patients (n = 27).

**C:** Kaplan-Meier survival analysis comparing normal and deregulated DGC by log rank test. Censored data points are represented as vertical bars.

**D:** Ligand overlay assays performed with muscles from control and ACC patients.

**E:** Co-IPs performed with samples as in **D** with a skeletal actin antibody and subsequently immunoblotted for MyHC. Corresponding actin Western is shown.

Results also highlighted that wasting was not selective to the DGC, since similar deregulation occurred in actin-myosin complexes (Figure 8E). Nevertheless, these results demonstrate that gastrointestinal cancer patients exhibit dysfunctional DGC that correlates positively with cachexia and inversely with survival.

## Discussion

Cancer is often complicated by cachexia that interferes with treatment response and shortens survival (Tisdale, 2002). The findings in this study provide important insight into the mechanism of this disorder by revealing that tumor-induced DGC dysfunction is a contributing factor in muscle wasting. Although cancer cachexia and muscular dystrophy involve chronic muscle loss, from an etiological and molecular standpoint, the causative mechanisms of these disorders are considered to be largely nonoverlapping (McKinnell and Rudnicki, 2004). This is because muscular dystrophies are genetic in origin, with numerous mutations mapping to dystrophin and other DGC members. Moreover, dystrophy includes lymphocyte and macrophage recruitment, necrosis, muscle regeneration, apoptosis, and fibrosis that together culminate in a degenerative state (Campbell and Stull, 2003; Dalkilic and Kunkel, 2003). In contrast, a genetic disposition for muscle wasting in cancer has not been described, and biopsies from carcinoma patients and a murine model presented here reveal little if any evidence of infiltrating cells, necrosis, regeneration, apoptosis, or fibrosis. Rather, muscle loss due to malignancy exhibits pronounced fiber atrophy and increased vascularization, which most likely serves to facilitate circulation of tumor factors and host cytokines in the microenvironment.

Despite differences between cachexia and muscular dystrophy, our findings indicate that one potentially important commonality is the abnormality of fiber membranes resulting from a deregulated DGC. Microscopy analysis revealed that muscle membranes from cachectic mice were highly wrinkled and irregular. Interestingly, irregularities of membranes have also been reported in DMD patients as secondary consequences of DGC dysfunction (Mokri and Engel, 1975). In dystrophy, DGC mutations are thought to weaken membranes, measured by EBD uptake and CK release (Durbeej and Campbell, 2002). In muscles from C-26 mice, EBD membrane association was clearly visible, but only on a few occasions did the dye accumulate in the cytoplasm, and CK release was rarely noted. This indicates that alterations in fiber membranes occur in cachectic fibers, but to a lesser degree than in dystrophic muscles. We speculate that this difference in damage correlates with the degree of dysfunction exhibited by the DGC. In DMD, loss of dystrophin leads to a reduction of DG and SG proteins, resulting in the functional breakdown of the DGC (Blake et al., 2002). In the C-26 model, dystrophin expression is reduced but not eliminated, and the loss of other DGC proteins is not observed. Nevertheless, evidence from *mdx* and dystrophin transgenic mice indicates that alterations in the DGC from developing tumors are sufficient to induce membrane damage that may function as a cause and not simply a consequence of muscle atrophy. Gastrointestinal cancers, specifically gastroesophageal ACC, are the most highly associated with cachexia and have the fastest increasing incidence of any solid tumor in Europe and America (Lagergren, 2005). Given the extent to which dystrophin was reduced in patients with these types of cancers, it will be interesting to examine how this regulation impacts the expression of other DGC members and the overall integrity of muscle membranes.

In conjunction with dystrophin regulation, two other members of the DGC, β-DG and β-SG, were aberrantly glycosylated in tumor cachexia models and cachectic patients. Results showing that such glycosylation also occur in *mdx* muscle is genetic evidence that loss of dystrophin expression leads to aberrant glycosylation in DGC proteins. The data further revealed that DGC deregulation correlated with a significant loss in binding among DGC members. We suspect that the decrease in dystrophin contributes to the reduction in these in-

teractions, but further studies are warranted to determine if aberrant glycosylation also contributes to DGC dysfunction and muscle wasting. In certain congenital dystrophies, mutations in glycosyltransferases decrease rather than increase glycosylation of DGC proteins (Michele et al., 2002). However, transgenic expression of a glycosyltransferase in muscle was also shown to reduce fiber diameters (Xia et al., 2002). Thus, it is possible that increases in glycosyltransferase activity in tumor-bearing mice may be a contributing factor in cachexia.

It is not known at this time whether tumor-induced DGC dysfunction leads to muscle wasting via a breakdown in the mechanical link between the extracellular matrix and the cytoskeletal network, or through a disruption in the signaling link between the DGC and MAP kinase or the PI(3)K/Akt pathways (Rando, 2001). Data showing that β-DG/Grb2 interactions, as well as Erk and Akt activities, are maintained in cachectic muscles support a connection between a disrupted mechanical link and muscle atrophy. However, it is equally likely that tumor-induced alterations in the DGC may abrogate a separate, yet to be identified pathway that is critical to promote wasting. Such a pathway could be the proteasome system, since studies have established the requirement of muscle-specific E3 ligases, MuRF1 and atrogin-1/MAFBx, in several cachectic states (Jackman and Kandarian, 2004). Induction of these genes leads to polyubiquination and degradation of key skeletal muscle proteins such as MyHC (Acharyya et al., 2004). Data showing that MyHC reduction was accentuated in *mdx* mice with tumors while muscle atrophy and E3 ubiquitin ligase induction were blocked in dystrophin transgenic animals argue for a role of a dysfunctional DGC in proteasome regulation. Since results indicate that tumor reduction of dystrophin is posttranscriptional, it is also possible that activation of the proteasome may regulate dystrophin by a feedback mechanism.

Our results support a model in which, during tumor progression, circulating factors function to reduce dystrophin levels, leading to aberrant glycosylation of β-DG and β-SG proteins. These events promote DGC breakdown followed by membrane abnormalities. A dysfunctional DGC, either alone or in combination with other deregulated factors associated with an altered membrane or basal lamina, in turn stimulates the induction of E3 ligase genes and possibly other components of the proteasome pathway, culminating in a cachectic state. Since results showed that E3 ligase induction was not completely blocked in tumor-bearing dystrophin transgenic muscle, while NF-κB remained activated, this model also predicts that activation of the proteasome pathway is likely to be dependent on multiple pathways elicited from tumor and cytokine signaling receptors.

Collectively, evidence in this study suggests that DGC dysfunction is an important step in cancer cachexia. Since effective therapies are currently lacking, results also imply that approaches targeted to restore the DGC in muscular dystrophies could also be considered as a viable option in designing anticancer cachexia therapy.

## Experimental procedures

### Mice

Male CD2F1 (BALB/c × DBA/2) mice weighing 22–24 g were used, and C-26 cells were subcutaneously injected in the right flank as described (Acharyya et al., 2004). *mdx* mice (C57BL/10 ScSn DMD$^{mdx}$) and Δ17-48 (CVBA 3′) dystrophin transgenic mice (Phelps et al., 1995) were crossed into a CD2F1 background up to six generations. Mice were housed in the animal facility at The Ohio State University Comprehensive Cancer Center under conventional conditions with constant temperature and humidity and fed a standard diet. Treatment of mice was in accordance with the institutional guidelines of The Ohio State University Animal Care and Use Committee. For LLC cachexia, 5 × $10^5$ LLC cells were intramuscularly injected into quadriceps.

### Histology and electron microscopy

Muscles were sectioned at 10 μM on a cryostat (Leica) and stained with H&E or with myofibrillar ATPase (pH 4.2 or pH 4.6). Fiber measurements were obtained from a minimum of 1500 fibers per five to six randomly chosen fields and recorded from the shortest diameter using Axiovision 3.1 software (Zeiss). For EM, muscles were stretched in situ with bone support, fixed in 3% glutaraldehyde in 0.1 M PBS, and sectioned for analysis on a Phillips CM 12 microscope as described (Sahenk and Mendell, 1979). Dystrophic calcifications were detected by von Kossa calcium staining (Bodensteiner and Engel, 1978).

### Vital staining with EBD

EBD was injected intraperitoneally at 1 mg/10 g body weight. After 24 hr, mice were sacrificed, and muscles were frozen in liquid nitrogen-cooled isopentane. Frozen sections were mounted with Antifade reagent (Biomeda) and observed under a fluorescent microscope. CK assays were performed as described by the manufacturer (Pointe Scientific Inc).

### Immunostaining

Immunofluorescence and immunohistochemistry were performed as previously described, respectively (Phelps et al., 1995; Hertlein et al., 2005). Antibodies used were dystrophin (1:40), β-DG (1:200), and β-SG (1:200) from Novocastra; utrophin (1:100) from BD Pharmingen; von Willebrand factor (1:300) from Dako; and laminin (1:150) and MyHC I (1:500) from Sigma. TUNEL assays were performed as described by the manufacturer (Roche).

### LCM

Approximately 5000 muscle fibers per group were laser captured using a Pixcell II LCM system (Arcturus Engineering) from frozen muscle sections. Fibers were lysed in 15 μl of a lysis solution containing 1:1 mixture of SDS electrophoresis sample buffer and mammalian protein extraction reagent (Pierce Biotechnology) and subsequently analyzed by Westerns.

### Western blot, coimmunoprecipitation, and EMSA

Western and coimmunoprecipitations were performed as previously described (Acharyya et al., 2004), with the exception that α-DG incubations were done with 150 mM NaCl, 20 mM Tris (pH 7.4). Antibodies used were dystrophin (dys-2;1:50), β-DG (1:100), α-SG (1:200), β-SG (1:200), and dysferlin (1:100) from Novocastra; utrophin (1:250), Grb2 (1:5000), and β-DG (clone 56; 1:500) from BD Pharmingen; α-DG (IIH6; 1:5000) from K. Campbell (University of Iowa); β-DG (MANDAG 2; 1:100) from G. Morris (North East Wales Institute); MyHC I and II, actin, troponin, tropomyosin, α-tubulin (1:1000), laminin (1:500), and syntrophin (1:1000) from Sigma; caveolin-3 (1:2500) from Research Diagnostics Inc.; ATPase β1 (1:50) and NCAM (1:50) from Developmental Hybridoma Bank; Akt (1:5000), phospho-Akt Ser-473 (1:2000), phospho-p70S6K Thr-389, p70S6K, phospho ERK Thr-202/Tyr-204, ERK, and phospho p65 Ser-536 from Cell Signaling; and p65 (1:10,000) from Rockland. Patient samples were probed with the 18.4 dystrophin rabbit polyclonal antibody (1:50,000) specific to the carboxy terminus (Cox et al., 1994). For enzymatic deglycosylation and dephosphorylation analysis, 20 μg of tissue lysate was treated with PNGase F or λ phosphatase (New England Biolabs) respectively, as recommended by the manufacturer. EMSA was performed as described (Kumar and Boriek, 2003).

### Laminin overlay assays

Laminin overlay assays were performed with 500 μg of muscle lysates and incubated overnight at 4°C with 30 μl of wheat germ agglutinin (WGA)-agarose beads (Vector Labs) as previously described (Michele et al., 2002).

### Northern blot and real-time PCR

Northern blots and real-time PCR were performed as described (Hertlein et al., 2005) with the following primers: CD68, 5′-ACAGGCAGCACAGTGGA

CATTC-3′ forward, 5′-ATGATGAGAGGCAGCAAGAGGG-3′ reverse; control GAPDH, 5′-GCAAATTCAACGGCACAGTCAAG-3′ forward, 5′-GGTAC AAACACTACCCACACTTG-3′ reverse.

**Grip strength measurement**

Total grip strength was measured from control and tumor-bearing mice (21–22 days after injection) using a Digital Grip Strength Meter (Columbus Instruments). A minimum of three measurements was taken from each mouse. Hindlimb grip strength was calculated as the difference between total and forelimb grip strengths. The observer (M.E.R.B.) was blinded to the genotype of the mice.

**Patients**

Muscle biopsies (abdominus rectus) were obtained from men and nonpregnant women between 18 and 80 years of age with informed patient consent. Diagnosis was based on histological or unequivocal radiological or operative findings. Healthy, weight-stable subjects undergoing minor surgical procedures (e.g., inguinal hernia repair) were included in this study. Venous blood sampling was performed, and serum C-reactive protein was analyzed by an automated immunoturbidometric method (Abbott Diagnostics). Body weight was measured with subjects in light clothing without shoes using a beam scale (Seca). Survival was recorded from the time of initial diagnosis. Studies involving human subjects were done in accordance with the Lothian Ethical Committee (UK) and the Institutional Review Boards of the Universities of Nebraska and Ohio State.

**Statistical analysis**

All quantitative data are represented as mean ± SEM. Analysis was performed between different groups using a two-tailed Student's t test for fiber diameter quantitation. One-way analysis of variance was performed with Bonferroni post hoc comparison using SPSS V13 for muscle mass and grip strength quantitation. Statistical significance was set at a p value of $<0.05$.

**Supplemental data**

The Supplemental Data include five supplemental figures and one supplemental table and can be found with this article online at http://www.cancercell.org/cgi/content/full/8/5/421/DC1/.

**Acknowledgments**

We appreciate assistance provided by OSU microscopy, histology, and mouse phenotyping cores. Special thanks go to members of the OSU neuromuscular laboratory, I. Kakabadze, S. Cai, and J. Stein, and J. Anderson at the University of Nebraska. We also thank K. Campbell for α-DG antibody; J. Chamberlain for dystrophin antibody; G. Morris for β-DG antibody; and M. Weinstein, V.K. Bergdall, M. Belury, P. Reiser, P. Kaumaya, and S.R. Hussein for technical advice. Special appreciation is also extended to members of the Guttridge laboratory, especially E. Hertlein, J. Wang, K. Ladner, and N. Bakkar for assistance and helpful discussions. This work was funded by NIH grants CA097953, CA098466, and CA72712 and by the V Foundation.

Received: February 9, 2005
Revised: August 13, 2005
Accepted: October 12, 2005
Published: November 14, 2005

**References**

Acharyya, S., Ladner, K.J., Nelsen, L.L., Damrauer, J., Reiser, P.J., Swoap, S., and Guttridge, D.C. (2004). Cancer cachexia is regulated by selective targeting of skeletal muscle gene products. J. Clin. Invest. *114*, 370–378.

Andreyev, H.J., Norman, A.R., Oates, J., and Cunningham, D. (1998). Why do patients with weight loss have a worse outcome when undergoing chemotherapy for gastrointestinal malignancies? Eur. J. Cancer *34*, 503–509.

Argiles, J.M., and Lopez-Soriano, F.J. (1999). The role of cytokines in cancer cachexia. Med. Res. Rev. *19*, 223–248.

Argiles, J.M., Moore-Carrasco, R., Fuster, G., Busquets, S., and Lopez-Soriano, F.J. (2003). Cancer cachexia: the molecular mechanisms. Int. J. Biochem. Cell Biol. *35*, 405–409.

Badorff, C., Lee, G.H., Lamphear, B.J., Martone, M.E., Campbell, K.P., Rhoads, R.E., and Knowlton, K.U. (1999). Enteroviral protease 2A cleaves dystrophin: evidence of cytoskeletal disruption in an acquired cardiomyopathy. Nat. Med. *5*, 320–326.

Blake, D.J., Weir, A., Newey, S.E., and Davies, K.E. (2002). Function and genetics of dystrophin and dystrophin-related proteins in muscle. Physiol. Rev. *82*, 291–329.

Bodensteiner, J.B., and Engel, A.G. (1978). Intracellular calcium accumulation in Duchenne dystrophy and other myopathies: a study of 567,000 muscle fibers in 114 biopsies. Neurology *28*, 439–446.

Bodine, S.C., Latres, E., Baumhueter, S., Lai, V.K., Nunez, L., Clarke, B.A., Poueymirou, W.T., Panaro, F.J., Na, E., Dharmarajan, K., et al. (2001). Identification of ubiquitin ligases required for skeletal muscle atrophy. Science *294*, 1704–1708.

Cai, D., Frantz, J.D., Tawa, N.E., Jr., Melendez, P.A., Oh, B.C., Lidov, H.G., Hasselgren, P.O., Frontera, W.R., Lee, J., Glass, D.J., and Shoelson, S.E. (2004). IKKβ/NF-κB activation causes severe muscle wasting in mice. Cell *119*, 285–298.

Campbell, K.P., and Stull, J.T. (2003). Skeletal muscle basement membrane-sarcolemma-cytoskeleton interaction minireview series. J. Biol. Chem. *278*, 12599–12600.

Chen, Y.W., Zhao, P., Borup, R., and Hoffman, E.P. (2000). Expression profiling in the muscular dystrophies: identification of novel aspects of molecular pathophysiology. J. Cell Biol. *151*, 1321–1336.

Cox, G.A., Sunada, Y., Campbell, K.P., and Chamberlain, J.S. (1994). Dp71 can restore the dystrophin-associated glycoprotein complex in muscle but fails to prevent dystrophy. Nat. Genet. *8*, 333–339.

Dalkilic, I., and Kunkel, L.M. (2003). Muscular dystrophies: genes to pathogenesis. Curr. Opin. Genet. Dev. *13*, 231–238.

Deans, C., and Wigmore, S.J. (2005). Systemic inflammation, cachexia and prognosis in patients with cancer. Curr. Opin. Clin. Nutr. Metab. Care *8*, 265–269.

Durbeej, M., and Campbell, K.P. (2002). Muscular dystrophies involving the dystrophin-glycoprotein complex: an overview of current mouse models. Curr. Opin. Genet. Dev. *12*, 349–361.

Ervasti, J.M., Ohlendieck, K., Kahl, S.D., Gaver, M.G., and Campbell, K.P. (1990). Deficiency of a glycoprotein component of the dystrophin complex in dystrophic muscle. Nature *345*, 315–319.

Esapa, C.T., Bentham, G.R., Schroder, J.E., Kroger, S., and Blake, D.J. (2003). The effects of post-translational processing on dystroglycan synthesis and trafficking. FEBS Lett. *555*, 209–216.

Farges, M.C., Balcerzak, D., Fisher, B.D., Attaix, D., Bechet, D., Ferrara, M., and Baracos, V.E. (2002). Increased muscle proteolysis after local trauma mainly reflects macrophage-associated lysosomal proteolysis. Am. J. Physiol. Endocrinol. Metab. *282*, E326–E335.

Glass, D.J. (2003). Signalling pathways that mediate skeletal muscle hypertrophy and atrophy. Nat. Cell Biol. *5*, 87–90.

Gomes, M.D., Lecker, S.H., Jagoe, R.T., Navon, A., and Goldberg, A.L. (2001). Atrogin-1, a muscle-specific F-box protein highly expressed during muscle atrophy. Proc. Natl. Acad. Sci. USA *98*, 14440–14445.

Guttridge, D.C., Mayo, M.W., Madrid, L.V., Wang, C.Y., and Baldwin, A.S., Jr. (2000). NF-κB-induced loss of MyoD messenger RNA: possible role in muscle decay and cachexia. Science *289*, 2363–2366.

Hasselgren, P.O., and Fischer, J.E. (2001). Muscle cachexia: current concepts of intracellular mechanisms and molecular regulation. Ann. Surg. *233*, 9–17.

Hertlein, E., Wang, J., Ladner, K.J., Bakkar, N., and Guttridge, D.C. (2005). RelA/p65 regulation of IκBβ. Mol. Cell. Biol. *25*, 4956–4968.

Hoffman, E.P., Brown, R.H., Jr., and Kunkel, L.M. (1987). Dystrophin: The

protein product of the Duchenne muscular dystrophy locus. Cell *51*, 919–928.

Holt, K.H., Crosbie, R.H., Venzke, D.P., and Campbell, K.P. (2000). Biosynthesis of dystroglycan: processing of a precursor propeptide. FEBS Lett. *468*, 79–83.

Hunter, R.B., and Kandarian, S.C. (2004). Disruption of either the Nfkb1 or the Bcl3 gene inhibits skeletal muscle atrophy. J. Clin. Invest. *114*, 1504–1511.

Jackman, R.W., and Kandarian, S.C. (2004). The molecular basis of skeletal muscle atrophy. Am. J. Physiol. Cell Physiol. *287*, C834–C843.

Jing, J., Lien, C.F., Sharma, S., Rice, J., Brennan, P.A., and Gorecki, D.C. (2004). Aberrant expression, processing and degradation of dystroglycan in squamous cell carcinomas. Eur. J. Cancer *40*, 2143–2151.

Karpati, G., and Carpenter, S. (2001). Pathology of Skeletal Muscle, Second Edition (New York: Oxford University Press).

Kumar, A., and Boriek, A.M. (2003). Mechanical stress activates the nuclear factor-κB pathway in skeletal muscle fibers: a possible role in Duchenne muscular dystrophy. FASEB J. *17*, 386–396.

Lagergren, J. (2005). Adenocarcinoma of oesophagus: what exactly is the size of the problem and who is at risk? Gut Suppl. *54*, i1–i5.

Lapidos, K.A., Kakkar, R., and McNally, E.M. (2004). The dystrophin glycoprotein complex: signaling strength and integrity for the sarcolemma. Circ. Res. *94*, 1023–1031.

Lecker, S.H., Solomon, V., Mitch, W.E., and Goldberg, A.L. (1999). Muscle protein breakdown and the critical role of the ubiquitin-proteasome pathway in normal and disease states. J. Nutr. *129*, 227S–237S.

Lecker, S.H., Jagoe, R.T., Gilbert, A., Gomes, M., Baracos, V., Bailey, J., Price, S.R., Mitch, W.E., and Goldberg, A.L. (2004). Multiple types of skeletal muscle atrophy involve a common program of changes in gene expression. FASEB J. *18*, 39–51.

Liu, Z., Wu, Y., Nicklas, E.W., Jahn, L.A., Price, W.J., and Barrett, E.J. (2004). Unlike insulin, amino acids stimulate p70S6K but not GSK-3 or glycogen synthase in human skeletal muscle. Am. J. Physiol. Endocrinol. Metab. *286*, E523–E528.

Marin, O.S., and Denny-Brown, D. (1962). Changes in skeletal muscle associated with cachexia. Am. J. Pathol. *41*, 23–39.

McKinnell, I.W., and Rudnicki, M.A. (2004). Molecular mechanisms of muscle atrophy. Cell *119*, 907–910.

Mendell, J.R., and Engel, W.K. (1971). The fine structure of type II muscle fiber atrophy. Neurology *21*, 358–365.

Michele, D.E., Barresi, R., Kanagawa, M., Saito, F., Cohn, R.D., Satz, J.S., Dollar, J., Nishino, I., Kelley, R.I., Somer, H., et al. (2002). Post-translational disruption of dystroglycan-ligand interactions in congenital muscular dystrophies. Nature *418*, 417–422.

Mokri, B., and Engel, A.G. (1975). Duchenne dystrophy: electron microscopic findings pointing to a basic or early abnormality in the plasma membrane of the muscle fiber. Neurology *51*, 1–10.

Ohlendieck, K., and Campbell, K.P. (1991). Dystrophin-associated proteins are greatly reduced in skeletal muscle from mdx mice. J. Cell Biol. *115*, 1685–1694.

Phelps, S.F., Hauser, M.A., Cole, N.M., Rafael, J.A., Hinkle, R.T., Faulkner, J.A., and Chamberlain, J.S. (1995). Expression of full-length and truncated dystrophin mini-genes in transgenic mdx mice. Hum. Mol. Genet. *4*, 1251–1258.

Rando, T.A. (2001). The dystrophin-glycoprotein complex, cellular signaling, and the regulation of cell survival in the muscular dystrophies. Muscle Nerve *24*, 1575–1594.

Reid, M.B., and Li, Y.P. (2001). Tumor necrosis factor-α and muscle wasting: a cellular perspective. Respir. Res. *2*, 269–272.

Rennie, M.J., Wackerhage, H., Spangenburg, E.E., and Booth, F.W. (2004). Control of the size of the human muscle mass. Annu. Rev. Physiol. *66*, 799–828.

Sahenk, Z., and Mendell, J.R. (1979). Ultrastructural study of zinc pyridinethione-induced peripheral neuropathy. J. Neuropathol. Exp. Neurol. *38*, 532–550.

Sandri, M., Sandri, C., Gilbert, A., Skurk, C., Calabria, E., Picard, A., Walsh, K., Schiaffino, S., Lecker, S.H., and Goldberg, A.L. (2004). Foxo transcription factors induce the atrophy-related ubiquitin ligase atrogin-1 and cause skeletal muscle atrophy. Cell *117*, 399–412.

Sicinski, P., Geng, Y., Ryder-Cook, A.S., Barnard, E.A., Darlison, M.G., and Barnard, P.J. (1989). The molecular basis of muscular dystrophy in the mdx mouse: a point mutation. Science *244*, 1578–1580.

Stitt, T.N., Drujan, D., Clarke, B.A., Panaro, F., Timofeyva, Y., Kline, W.O., Gonzalez, M., Yancopoulos, G.D., and Glass, D.J. (2004). The IGF-1/PI3K/Akt pathway prevents expression of muscle atrophy-induced ubiquitin ligases by inhibiting FOXO transcription factors. Mol. Cell *14*, 395–403.

Straub, V., Rafael, J.A., Chamberlain, J.S., and Campbell, K.P. (1997). Animal models for muscular dystrophy show different patterns of sarcolemmal disruption. J. Cell Biol. *139*, 375–385.

Temparis, S., Asensi, M., Taillandier, D., Aurousseau, E., Larbaud, D., Obled, A., Bechet, D., Ferrara, M., Estrela, J.M., and Attaix, D. (1994). Increased ATP-ubiquitin-dependent proteolysis in skeletal muscles of tumor-bearing rats. Cancer Res. *54*, 5568–5573.

Tinsley, J., Deconinck, N., Fisher, R., Kahn, D., Phelps, S., Gillis, J.M., and Davies, K. (1998). Expression of full-length utrophin prevents muscular dystrophy in mdx mice. Nat. Med. *4*, 1441–1444.

Tisdale, M.J. (2002). Cachexia in cancer patients. Nat. Rev. Cancer *2*, 862–871.

van Eys, J. (1985). Nutrition and cancer: physiological interrelationships. Annu. Rev. Nutr. *5*, 435–461.

Williams, A., Sun, X., Fischer, J.E., and Hasselgren, P.O. (1999). The expression of genes in the ubiquitin-proteasome proteolytic pathway is increased in skeletal muscle from patients with cancer. Surgery *126*, 744–749.

Xia, B., Hoyte, K., Kammesheidt, A., Deerinck, T., Ellisman, M., and Martin, P.T. (2002). Overexpression of the CT GalNAc transferase in skeletal muscle alters myofiber growth, neuromuscular structure, and laminin expression. Dev. Biol. *242*, 58–73.

Yoshida, M., and Ozawa, E. (1990). Glycoprotein complex anchoring dystrophin to sarcolemma. J. Biochem. (Tokyo) *108*, 748–752.